On the Distribution of Chemical Properties and Aggregation of Solubility Fractions in Asphaltenes

Keith L. Gawrys,† George A. Blankenship, and Peter K. Kilpatrick*

Department of Chemical and Biomolecular Engineering, North Carolina State University, Raleigh, North Carolina 27965-7905

Received July 5, 2005. Revised Manuscript Received January 12, 2006

Asphaltenes from B6, Canadon Seco (CS), and Hondo (HO) crude oils were separated on a preparatory scale into 20−30 so-called "fine fractions" by sequential precipitation from mixtures of *n*-heptane and toluene. Chemical analyses were performed to measure the carbon, hydrogen, nitrogen, sulfur, oxygen, and trace metals contents of the fractions. Small-angle neutron scattering (SANS) was performed on fractions dissolved or dispersed in mixtures of toluene-*d* (or methylnaphthalene-*d*) and methanol-*d* to determine the average aggregate size. Statistical analyses were performed to calculate the weighted moments of each elemental parameter assuming that the data were "normally" distributed. High values of the standard deviation and skewness because of the early precipitation of metal oxides and inorganic salts suggested that a Gaussian distribution was inappropriate to describe the behavior of most metals. H/C, N/C, and S/C ratios in B6 and HO asphaltenes appeared to obey a Gaussian distribution, with mean values approximating the average values for the whole asphaltenes. For CS asphaltenes, the initial 10% of precipitated material was generally less aromatic than the remaining fractions. Coefficients of linear correlation were calculated for the chemical composition, solubility, and aggregate size parameters and provided a statistical means of determining the properties of the asphaltene fractions that promoted aggregation and precipitation. Polar and hydrogen-bonding interactions appeared to be more important than dispersion interactions in the precipitation of B6 and HO asphaltenes. In particular, interactions of metalloporphyrins appeared to play a key role in the asphaltene aggregation mechanism. On the other hand, dispersion interactions likely dominated the solubility of CS asphaltenes.

Introduction

The tendency of petroleum asphaltenes to associate in solution and adsorb at interfaces can cause significant problems during the production, recovery, pipeline transportation, and refining of crude oil.[1−11] For example, a common method of increasing oil production involves the injection of miscible agents (e.g., carbon dioxide or natural gas) into underground reserves to displace the oil. This practice may result in the formation of asphaltene deposits that tend to plug up the reservoir wells and pipelines.[1,2,12] Similarly, asphaltene-stabilized water-in-crude oil (w/o) emulsions are formed during various stages of the production, such as by the turbulent flow of fluids up a bore hole, with the addition of "wash water" during the desalting operation, and by wave agitation of crude oil spills on water.[3−11] The propensity of asphaltenes to adsorb at interfaces is related to the extent of asphaltene aggregation and the solvating power of the crude oil media.[13] Asphaltenes maintain a delicate balance between solvency, aggregation, and interfacial activity in solution that must ultimately be related to the chemical composition and molecular architecture of the participating components.

Asphaltenes are defined as the portion of crude oil insoluble in light *n*-alkanes (e.g., *n*-heptane or *n*-pentane) but soluble in aromatic solvents (e.g., benzene or toluene).[14] The quantity, chemical composition, and molar mass distribution of the asphaltene "solubility class" varies significantly with the source of the crude oil and with the method of precipitation.[15−17] Asphaltenes comprise the most polar fraction of the crude oil and consist of polyaromatic condensed rings with short aliphatic side chains and polar heteroatom-containing functional groups.[18−22]

* To whom correspondence should be addressed. Telephone: (919) 515-7121. E-mail: peter-k@eos.ncsu.edu.

† Present address: Nalco Company, Sugar Land, TX 77478.

(1) Hammami, A.; Phelps, C. H.; Monger-McClure, T.; Little T. M. *Energy Fuels* **2000**, *14*, 14.

(2) Karan, K.; Hammami, A.; Flannery, M.; Stankiewicz, B. A. *Pet. Sci. Technol.* **2003**, *21*, 629.

(3) Taylor, S. D.; Czarnecki, J.; Masliyah, J. *J. Colloid Interface Sci.* **2002**, *252*, 149.

(4) Yarranton, H. W.; Hussein, H.; Masliyah, J. H. *J. Colloid Interface Sci.* **2000**, *228*, 52.

(5) Khristov, K.; Taylor, S. D.; Czarnecki, J.; Masliyah, J. *Colloids Surf., A* **2000**, *174*, 183.

(6) Havre, T. E.; Sjoblom, J. *Colloids Surf., A* **2003**, *228*, 131.

(7) Aske, N.; Kallevik, H.; Sjoblom, J. *Pet. Sci. Eng., J.* **2002**, *36*, 1.

(8) Aske, N.; Orr, R.; Sjoblom, J.; Kallevik, H.; Oye, G. *J. Dispersion Sci. Technol.* **2004**, *25*, 263.

(9) Auflem, I. H.; Kallevik, H.; Westvik, A.; Sjoblom, J. *Pet. Sci. Eng., J.* **2001**, *31*, 1.

(10) Spiecker, P. M.; Kilpatrick, P. K. *Langmuir* **2004**, *20*, 4022.

(11) Spiecker, P. M.; Gawrys, K. L.; Trail, C. B.; Kilpatrick, P. K. *Colloids Surf., A* **2003**, *220*, 9.

(12) Yang, X. L.; Kilpatrick, P. K. *Energy Fuels* **2005**, *19*, 1360.

(13) Spiecker, P. M.; Gawrys, K. L.; Kilpatrick, P. K. *J. Colloid Interface Sci.* **2003**, *267*, 178.

(14) Mitchell, D. L.; Speight, J. G. *Fuel* **1973**, *52*, 149.

(15) Brons, G.; Yu, J. M. *Energy Fuels* **1995**, *9*, 641.

(16) Miller, J. T.; Fisher, R. B.; Thiyagarajan, P.; Winans, R. E.; Hunt, J. E. *Energy Fuels* **1998**, *12*, 1290.

(17) McLean, J. D.; Kilpatrick, P. K. *Energy Fuels* **1997**, *11*, 570.

(18) Strausz, O. P.; Peng, P.; Murgich, J. *Energy Fuels* **2002**, *16*, 809.

(19) Sheremata, J. M.; Gray, M. R.; Dettman, H. D.; McCaffrey, W. C. *Energy Fuels* **2004**, *18*, 1377.

(20) Gray, M. R. *Energy Fuels* **2003**, *17*, 1566.

(21) Groenzin, H.; Mullins, O. C.; Eser, S.; Mathews, J.; Yang, M. G.; Jones, D. *Energy Fuels* **2003**, *17*, 498.

10.1021/ef0502002 CCC: $33.50
Published on Web 02/24/2006

Asphaltenes are polydisperse in chemical composition, with typical atomic H/C ratios varying between 1.0 and 1.3 and N, S, and O contents of a few weight percent.[13,23−25] Fourier transform infrared spectroscopy (FTIR) studies have shown that sulfur is evenly distributed among the acidic, basic, and neutral fractions of asphaltenes.[26−29] X-ray absorption near-edge structure spectroscopy (XANES) reveals that sulfur exists predominantly as thiophenic heterocycles and sulfidic groups.[30] The thiophenic groups are only slightly polar and are not likely to contribute to intermolecular associations, such as hydrogen-bonding. XANES studies also indicated the presence of small quantities of sulfoxides in asphaltenes obtained from biodegraded or partially oxidized crude oils. Unlike sulfur, oxygen- and nitrogen-containing moieties in asphaltenes are generally polar and capable of participating in strong intermolecular associations. For example, FTIR and XANES spectroscopy reveal several polar functional groups, such as carboxylic acids, carbonyls, phenols, pyrroles, and pyridines, that are capable of participating in proton donor−acceptor interactions.[29,31,32] Sjöblom and co-workers used diffuse reflectance FTIR to show that the interfacially active components of fractionated asphaltenes contained significant concentrations of acidic and open-chain carbonyl groups that introduce a strong hydrogen-bonding contribution to the mechanical film strength and prevent water-droplet coalescence.[33]

Various metals (e.g., Ni, V, Fe, Al, Na, Ca, and Mg) have also been shown to accumulate in the asphaltene fraction of crude oil, typically in concentrations much less than 1% (w/w).[13,17,34,35] Vanadium and nickel are generally the most abundant of the trace metals, are present to some extent as chelated porphyrin complexes, and have been linked to catalyst poisoning during the upgrading of heavy oils.[36−38] The concentrations of Fe, Al, Na, Ca, and Mg have also been reported to vary in deposits as a function of well depth[39] and among asphaltene fractions.[13,35]

Several of the above-described problems encountered during petroleum production may be related to or predominantly contributed to by a particular fraction of the total asphaltenes. Separation of the total asphaltenes into fractions is often motivated by an attempt to probe the relationship between the chemical composition, solubility, aggregation behavior, and emulsion-stabilizing properties of discrete portions of the asphaltene fraction. Previous methods of separating asphaltenes into fractions include gel-permeation chromatography,[40] sequential elution solvent chromatography,[41] liquid−liquid extraction,[42−44] dialysis fractionation,[45] ultracentrifugation,[46] and precipitation by the addition of flocculants.[13,21,32,34,35,42,47−50]

Two different experimental methods are common for the separation of asphaltenes into fractions by precipitation and will be referred to as the "coarse" and "fine" fractionation methods. The solvent/antisolvent combination used and exact procedure for the isolation of the precipitated asphaltenes generally varies between researchers; however, in both methods, the total asphaltene fraction is typically dispersed in a "good" solvent (e.g., toluene) at a fixed solute concentration and a flocculating solvent (e.g., *n*-heptane) is added to induce partial precipitation. During a coarse fractionation, two asphaltene fractions (i.e., insolubles and solubles) are isolated by asphaltene precipitation at a given solvent condition. Typically, the ratio of flocculant/solvent is varied, so that several pairs of more and less soluble fractions are isolated. For example, Yarranton and Masliyah studied the solubility behavior and molar mass distribution from vapor-pressure osmometry (vpo) and interfacial tension measurements of several Athabasca *n*-C_7 asphaltene coarse fractions precipitated from mixtures of *n*-hexane and toluene.[48] Andersen et al. isolated several coarse fractions of Boscan *n*-C_7 asphaltenes by precipitation in mixtures of *n*-heptane and toluene.[42,49] Spiecker et al. studied the solubility and aggregation behavior by small-angle neutron scattering (SANS) of coarse asphaltene fractions precipitated from various parent asphaltenes by a similar procedure.[13] In each of the above studies, the relative aromaticities, N/C contents, and aggregate sizes (in toluene or pyridine) of the less soluble fractions generally decreased with an increasing yield of precipitated asphaltenes (i.e., at higher flocculant/solvent ratios). Sulfur and oxygen contents were typically distributed evenly throughout the fractions. Furthermore, the less soluble fractions were generally more aromatic, had a higher N/C content, and formed larger aggregates in toluene and pyridine than the more soluble fractions.

Instead of generating only two fractions, one of which represents at least half of the original asphaltenes by mass, the fine fractionation procedure here separates the total asphaltenes into several discrete fractions by a stepwise increase in the concentration of the flocculating solvent. During each precipitation step, a small amount of asphaltene material is precipitated

(22) Bergmann, U.; Groenzin, H.; Mullins, O. C.; Glatzel, P.; Fetzer, J.; Cramer, S. P. *Pet. Sci. Technol.* **2004**, *22*, 863.
(23) Bestougeff, M. A. *Bull. Soc. Chim. Fr.* **1967**, *12*, 4773.
(24) Boduszynski, M. M. *Prepr. ACS Div. Pet. Chem.* **1985**, *30*, 626.
(25) Boduszynski, M. M. *Energy Fuels* **1988**, *2*, 597.
(26) McKay, J. F.; Harnsberger, P. M.; Erickson, R. B.; Cogswell, T. E.; Latham, D. R. *Fuel* **1981**, *60*, 17.
(27) McKay, J. F.; Amend, P. J.; Harnsberger, P. M.; Cogswell, T. E.; Latham, D. R. *Fuel* **1981**, *60*, 14.
(28) McKay, J. F.; Latham, D. R.; Haines, W. E. *Fuel* **1981**, *60*, 27.
(29) Boduszynski, M. M.; McKay, J. F.; Latham, D. R. *Proc. Assoc. Asphalt Paving Technol.* **1980**, *49*, 123.
(30) Mullins, O. C. Sulfur and Nitrogen Molecular Structures in Asphaltenes and Related Materials Quantified by XANES Spectroscopy. In *Asphaltenes: Fundamentals and Applications*; Mullins, O. C., Ed.; Plenum Press: New York, 1995; p 53.
(31) Mitrakirtley, S.; Mullins, O. C.; Vanelp, J.; George, S. J.; Chen, J.; Cramer, S. P. *J. Am. Chem. Soc.* **1993**, *115*, 252.
(32) Buenrostro-Gonzalez, E.; Andersen, S. I.; Garcia-Martinez, J. A.; Lira-Galeana, C. *Energy Fuels* **2002**, *16*, 732.
(33) Mingyuan, L.; Christy, A.; Sjoblom, J. Water-in-Crude Oil Emulsions from the Norwegian Continental Shelf Part VI−Diffuse Reflectance Fourier Transform Infrared Characterization of Interfacially Active Fractions from North Sea Crude Oil. In *Emulsions: A Fundamental and Practical Approach*; Sjoblom, J., Ed.; Kluwer Academic Publishers: Dordrecht, The Netherlands, 1992; p 157.
(34) Kaminski, T. J.; Fogler, H. S.; Wolf, N.; Wattana, P.; Mairal, A. *Energy Fuels* **2000**, *14*, 25.
(35) Yang, X. L.; Hamza, H.; Czarnecki, J. *Energy Fuels* **2004**, *18*, 770.
(36) Ali, M. F.; Perzanowski, H.; Bukhari, A.; Al-Haji, A. A. *Energy Fuels* **1993**, *7*, 179.
(37) Ovalles, C.; Rojas, I.; Acevedo, S.; Escobar, G.; Jorge, G.; Gutierrez, L. B.; Rincon, A.; Scharifker, B. *Fuel Process. Technol.* **1996**, *48*, 159.
(38) Pena, M. E.; Manjarrez, A.; Campero, A. *Fuel Process. Technol.* **1996**, *46*, 171.
(39) Chouparova, E.; Lanzirotti, A.; Feng, H.; Jones, K. W.; Marinkovic, N.; Whitson, C.; Philp, P. *Energy Fuels* **2004**, *18*, 1199.
(40) Cyr, N.; McIntyre, D. D.; Toth, G.; Strausz, O. P. *Fuel* **1987**, *66*, 1709.
(41) Jacobs, F. S.; Filby, R. H. *Fuel* **1983**, *62*, 1186.
(42) Andersen, S. I.; Keul, A.; Stenby, E. *Pet. Sci. Technol.* **1997**, *15*, 611.
(43) Ostlund, J. A.; Wattana, P.; Nyden, M.; Fogler, H. S. *J. Colloid Interface Sci.* **2004**, *271*, 372.
(44) Ostlund, J. A.; Nyden, M.; Fogler, H. S.; Holmberg, K. *Colloids Surf., A* **2004**, *234*, 95.
(45) Acevedo, S.; Escobar, G.; Ranaudo, M. A.; Pinate, J.; Amorin, A.; Diaz, M.; Silva, P. *Energy Fuels* **1997**, *11*, 774.
(46) Fenistein, D.; Barre, L. *Fuel* **2001**, *80*, 283.
(47) Nalwaya, V.; Tangtayakom, V.; Piumsomboon, P.; Fogler, S. *Ind. Eng. Chem. Res.* **1999**, *38*, 964.
(48) Yarranton, H. W.; Masliyah, J. H. *AIChe J.* **1996**, *42*, 3533.
(49) Andersen, S. I. *Fuel Sci. Technol. Int.* **1994**, *12*, 1551.
(50) Andersen, S. I. *Fuel Sci. Technol. Int.* **1995**, *13*, 579.

Table 1. Hansen Partial Solubility Parameter Values of Selected Solvents[54]

solvent	δ_d (MPa)$^{1/2}$	δ_p (MPa)$^{1/2}$	δ_h (MPa)$^{1/2}$	δ (MPa)$^{1/2}$
n-pentane	14.5	0.0	0.0	14.5
n-heptane	15.3	0.0	0.0	15.3
toluene	18.0	1.4	2.0	18.2
acetone	15.5	10.4	7.0	19.9
methylene chloride	18.2	6.3	6.1	20.2

and isolated, the soluble filtrate is recovered, and the next fraction is precipitated after a change in solvent conditions. The major difference between the coarse and fine fractionation methods is that the coarse fractions that precipitated at higher flocculant contents likely contain the entire subset of chemical species present in fractions precipitated at lower flocculant contents; whereas each fine fraction should represent the discrete subset of asphaltenes that precipitate within the range of two solvent conditions. For example, Yang et al. isolated six asphaltene fractions from Athabasca bitumen by stepwise increasing the ratio of *n*-heptane/bitumen (H/B).[35] The first fraction to precipitate was the most aromatic and had the highest concentration of Fe, Ca, Mg, and Al. The atomic H/C ratio was observed to increase, and metalloporphyrin contents decrease systematically as the fractionation proceeded (i.e., at higher H/B ratios). Unlike the previous analyses of coarse fractions by SANS and vpo,[13,48] no significant variations in aggregate molar mass were observed by vpo for the fractions dissolved in toluene at 50 °C. Groenzin et al. isolated six fractions of *n*-C_5 asphaltenes by sequential precipitation in mixtures of *n*-pentane and toluene.[21] Fluorescence depolarization measurements on solutions of the asphaltene fractions in toluene indicated that the less soluble fractions emitted at higher wavelengths than more soluble fractions, possibly suggesting that the less soluble fraction contained a higher population of larger chromophores.

Asphaltene precipitation at a given solvent condition may be related to specific intermolecular forces (i.e., dispersion, polar, and hydrogen bonding) using the multicomponent solubility parameter concept.[51−53] Table 1 compares the Hansen partial solubility parameters for selected solvents, including *n*-heptane, *n*-pentane, and toluene.[54] As indicated in the table, increasing the amount of *n*-heptane or *n*-pentane flocculant during the above-described fractionation experiments mainly varied the dispersion contribution to the overall solubility parameter. Buenrostro-Gonzalez et al. compared the chemical composition of fractions isolated by stepwise increasing the amount of flocculant (i.e., acetone or *n*-heptane) added to a 2.3% (w/w) solution of Mayan *n*-C_7 asphaltenes in toluene.[32] The replacement of *n*-heptane with acetone introduced significant polar and hydrogen-bonding contributions to the solvent character. A total of 10 discrete fractions were isolated for each solvent mixture, but not enough material was precipitated during the first few fractionations (i.e., the least soluble asphaltene fractions) to perform subsequent chemical analyses. There were no apparent trends in atomic H/C, N/C, S/C, or O/C with the order of fractionation for the heptane/toluene fractions analyzed. Similarly, there were no apparent trends in atomic H/C, N/C, or S/C for the acetone/toluene fractions; however, the O/C content appeared to increase continuously from the third to sixth fraction. These results suggested that polar and hydrogen-bonding interactions dominated the solubility behavior at low acetone contents, while dispersion interactions dominated the solubility behavior at high acetone contents and for the heptane/toluene fractions. Similar fractionations performed by Fogler and coworkers were completed by sequentially increasing the amount of *n*-pentane flocculant to a mixture of Mobil and Venezuelan *n*-C_7 asphaltenes in methylene chloride.[34,47] Marked differences in physical appearance, crystallinity, and solubility behavior (in dodecylbenzene sulfonic acid) were observed between the most polar and least polar fractions. Similarly, the more polar fractions had higher metals contents (i.e., Fe, Ni, and V) than the least polar fraction.

(51) Redelius, P. *Fuel* **2000**, *79*, 27.
(52) Karlsson, R.; Isacsson, U. *Energy Fuels* **2003**, *17*, 1407.
(53) Redelius, P. *Energy Fuels* **2004**, *18*, 1087.
(54) Hansen, C. M. *Hansen Solubility Parameters: A User's Handbook*; CRC Press: Boca Raton, FL, 1999.

Table 2. Crude Oil and Whole Asphaltene Properties

crude	weight % asphaltene	R/A ratio	viscosity (cP), 100 °F	H/C asphaltene	N/C asphaltene	H/C resin
B6	13.1	0.92	2030	1.22	0.0201	1.51
CS	7.5	1.19	70	1.11	0.0190	1.39
HO	14.8	1.39	363	1.24	0.0236	1.51

In the current study, the fractionation of asphaltenes is expanded to the isolation of 20−30 asphaltene fine fractions per crude oil [i.e., Hondo (HO), B6, and Canadon Seco (CS)], with typical fractions representing ∼1−18% of the total asphaltenes by mass. The various fine fractions were isolated by precipitation of asphaltenes from mixtures of *n*-heptane and toluene. Combustion elemental analyses and ICP metals analyses were performed to measure the carbon, hydrogen, nitrogen, sulfur (B6 only), oxygen (B6 only), and trace metals contents of each fraction. SANS measurements were performed on all of the HO and B6 fractions dissolved in mixtures of toluene-*d* (or methylnaphthalene-*d*) and methanol-*d*. The objective of the preparatory-scale separation of the asphaltenes into several discrete fractions and subsequent analyses was to identify the specific chemical properties responsible for asphaltene precipitation at a given solubility parameter.

Experimental Section

Materials. Asphaltenes were isolated from three crude oils identified as B6, HO, and CS. HO and B6 crude oils were obtained from off-shore California. CS crude oil was obtained from Argentina. The crude oils were asphaltene-rich and varied in viscosity, resin/asphaltene (R/A) mass ratio, and asphaltene chemical composition. Physical and chemical properties of the crude oils and isolated asphaltenes are summarized in Table 2. Asphaltene isolation and fractionation experiments were performed using toluene, *n*-heptane, and methylene chloride (HPLC grade) obtained from Fisher Scientific. The deuterated solvents used in SANS experiments (i.e., toluene-*d*, methylnaphthalene-*d*, and methanol-*d*) were obtained from CDN Isotopes and had >99.9% chemical purity and >99.5% perdeuteration.

Asphaltene Precipitation. Asphaltenes were precipitated from the corresponding source crude oils by the addition of excess *n*-heptane (40:1, v/v). The crude oil/*n*-heptane mixtures were subjected to 24 h of constant, gentle shaking to ensure that all of the material was completely dispersed. After this equilibration period, the precipitated asphaltenes were removed by vacuum filtration through 15 cm diameter, 1.5 μm Whatman 934-AH glass microfiber filter paper. The filter cake was rinsed with an excess of *n*-heptane to remove coprecipitated maltenes. The filter cake (i.e., precipitated asphaltenes) was completely dissolved from the filter paper and recovered in a different collection flask by the addition of excess methylene chloride under partial vacuum. Most of the solvent was removed from the asphaltene solutions by rotary evaporation under partial vacuum at 40 °C. Once nearly dry, the asphaltenes were moved into a nitrogen-flushed vacuum oven at 50 °C for 24 h. The dry asphaltenes were transferred to glass jars and stored under argon to prevent oxidation. The asphaltenes that

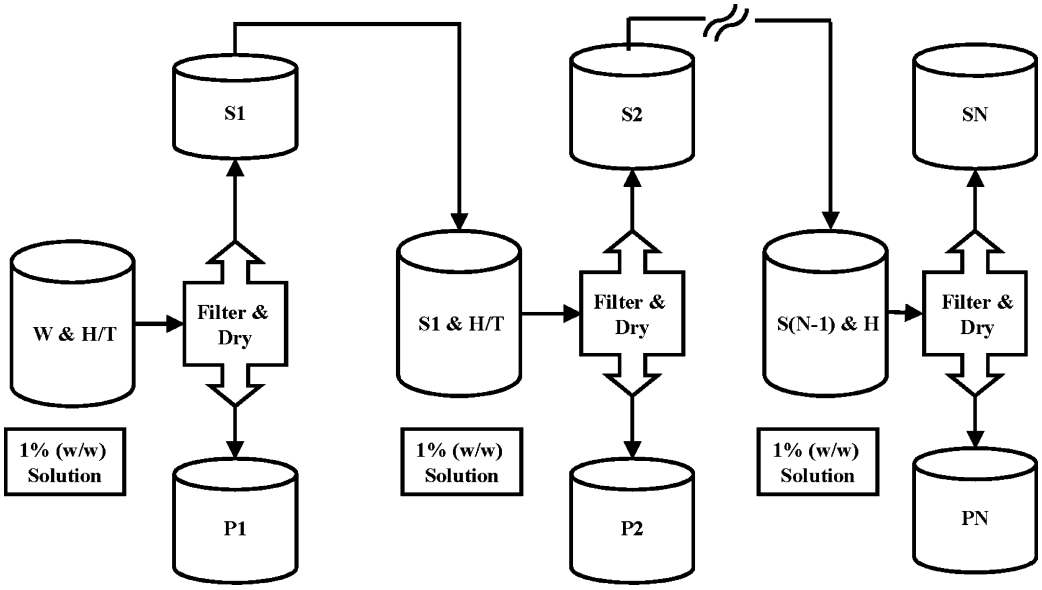

Figure 1. Schematic representation of the fine fractionation procedure for the preparation of *N* fractions. Whole asphaltenes (W) are dispersed in mixtures of heptane and toluene (H/T) at a fixed solute concentration. After filtration of the equilibrated solution, the filter cake (P1) and filtrate (S1) are recovered and dried. The S1 fraction is dispersed in a H/T mixture with a higher heptane volume fraction to recover a second precipitated fraction (P2). The sequential fractionation of the soluble fraction (S2) continues until *N* fractions are isolated. The final precipitated fraction (PN) and soluble fraction (SN) are isolated from pure heptane.

were isolated from the crude oils by the above method will be referred to as the "whole" asphaltenes for the remainder of the text.

Desalting of B6 Asphaltenes. The whole B6 asphaltenes precipitated according to the above procedure were suspected to contain coprecipitated inorganic salts, because the source crude oil was sampled from the bottom of a 5 gallon drum containing a mixture of crude oil and sedimented seawater. Spiecker et al. observed a relatively high concentration of sodium in whole B6 asphaltenes (9300 ppm) and a fraction of B6 asphaltenes that was insoluble in 60:40 *n*-heptane/toluene (25 000 ppm) obtained from the same crude oil source used in this study.[13] The Na content in the whole B6 asphaltenes was reduced from 9300 to 35 ppm by extracting a crude oil/methylene chloride mixture with deionized water prior to the asphaltene precipitation. The reduction in Na content suggested that the B6 asphaltenes contained either co-precipitated inorganic salts (e.g., NaCl) or water-soluble soaps of corresponding carboxylic acids. In this study, a similar desalting procedure was followed for the whole B6 asphaltenes prior to the fine fractionation steps. Whole B6 asphaltenes were dissolved in methylene chloride (1 g/100 mL) and extracted with a 0.1 M solution of HCl. The organic and aqueous phases were intermingled in a 500 mL separatory funnel in a 1:1 ratio (v/v). The addition of HCl was expected to increase the surface area of contact between the organic and aqueous phases by the formation of a weak emulsion that could be broken by gravity settling. After the acid extraction, the organic phase was extracted with deionized water (3×). The whole B6 asphaltenes were recovered from the organic phase by rotary evaporation of the methylene chloride solvent and subsequent drying in the vacuum oven according to the procedure described above.

Asphaltene Fine Fractionation. The whole HO, CS, and desalted B6 asphaltenes were further separated into several fractions by sequential fractionation in mixtures of *n*-heptane and toluene. A schematic representation of the fine fractionation procedure is shown in Figure 1. During the fractionations, approximately 20 g of whole asphaltenes were dissolved in the toluene solution such that the total asphaltene concentration was 1% (w/w) after flocculant addition. Upon dissolution in toluene, enough *n*-heptane was added to the solution to induce partial precipitation of approximately 1−2% of the whole asphaltenes. The asphaltene solutions were subjected to 24 h of constant, gentle shaking to allow for equilibration of the samples. The precipitated asphaltenes were isolated by vacuum filtration and recovered similarly to the above-described procedure for asphaltene precipitation. The precipitated asphaltenes became the first fine fraction, P1. The soluble asphaltenes were recovered from the filtrate (S1 fraction) by rotary evaporation and dried in a nitrogen-flushed vacuum oven at 50 °C for 24 h. The S1 fraction was then dispersed in a mixture of toluene and *n*-heptane containing a higher concentration of flocculant according to the above procedure, such that another 1−2% of the whole asphaltenes was precipitated. The fractionation procedure continued using progressively more *n*-heptane as a flocculant until 20−30 fine fractions were isolated. During the final fractionation step, the soluble asphaltenes from the previous fraction were dispersed in pure *n*-heptane to obtain a precipitated fraction (i.e., PN in Figure 1) and an *n*-heptane-soluble fraction (i.e., SN).

Chemical Characterization. The B6 asphaltene fractions were characterized by combustion elemental analysis (carbon, hydrogen, nitrogen, sulfur, and oxygen) at the University of Alberta (Department of Chemistry, Edmonton, Alberta, Canada) using a Carlo Erba instrument. The HO and CS asphaltene fractions were characterized by combustion elemental analysis (carbon, hydrogen, and nitrogen) at Nalco Energy Services (Sugar Land, TX). Metals analyses for all of the asphaltene fractions were performed at the Nalco Energy Services using a Jerrel Ash 9000 by the ICP technique.

SANS. Solutions with a mass concentration of 1% (w/w) were prepared by dissolving various asphaltene fine fractions in mixtures of toluene-*d*, methylnaphthalene-*d*, and methanol-*d*. During the sample preparation, toluene-*d* or methylnaphthalene-*d* was initially added to the dry asphaltenes and the solution was subjected to constant, gentle shaking until the asphaltenes were completely dissolved. Upon dissolution of the asphaltenes, methanol-*d* was added to the solutions. The solutions were allowed to equilibrate for at least 1 week prior to performing the scattering experiments. SANS measurements were performed on all of the HO fine fractions in 90:10 toluene-*d*/methanol-*d* (v/v), all of the B6 fine fractions in 90:10 methylnaphthalene-*d*/methanol-*d* (v/v), and the most soluble 30% (w/w) of the B6 fine fractions in toluene-*d*. In previous studies, it was observed that the addition of a small amount of methanol-*d* to solutions of asphaltenes in toluene-*d* (or methylnaphthalene-*d*) was sufficient to disrupt interactions between polar heteroatoms within the aggregates and reduce the aggregate size.[55] Because

(55) Gawrys, K. L.; Kilpatrick, P. K. *J. Colloid Interface Sci.* **2005**, *288*, 325.

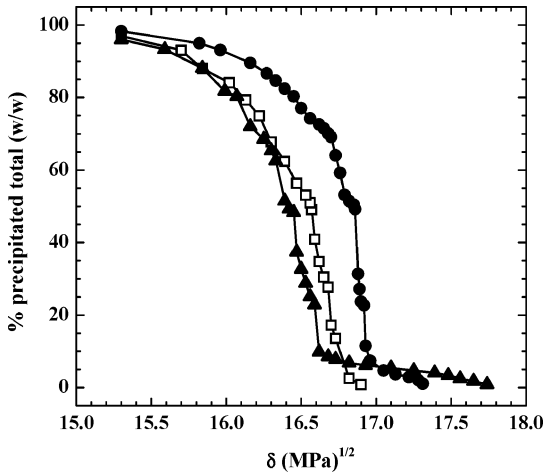

Figure 2. Cumulative percentages of asphaltenes precipitated as function of the total solvent solubility parameter, δ, for (filled triangles) CS, (open squares) HO, and (filled circles) B6 asphaltenes in mixtures of *n*-heptane and toluene.

several of the earliest fractions isolated were insoluble in toluene-*d* and methylnaphthalene-*d*, a small amount of methanol-*d* was added to the mixtures to enable dissolution of the asphaltenes.

Most of the SANS measurements were performed on the small-angle neutron diffractometer (SAND) at the Intense Pulsed Neutron Source Division of the Argonne National Laboratory (Argonne, IL); however, additional experiments were performed on the 30 m NG3 and 8 m NG1 small-angle spectrometers at the National Institute of Standards and Technology (NIST) Center for Neutron Research (Gaithersburg, MD). The SAND instrument at the Argonne National Laboratory is a time-of-flight diffractometer attached to an accelerator-based pulsed neutron source (30 Hz). Each pulse contains neutrons with wavelengths ranging from 1 to 14 Å. The higher energy neutrons had lower wavelengths and reached the sample ahead of the lower energy neutrons. Thus, the energy of each scattered neutron was determined by its "time-of-flight" to the detector. The available Q range for the SAND instrument extended from 0.0035 to 2 $Å^{-1}$. During the NG3 and NG1 (NIST) experiments, the source−sample distance was varied from 4 to 16 m, while the sample−detector distance was varied from 1.2 to 15 m. Neutrons of 6 Å wavelength and 0.22 spread ($\Delta\lambda/\lambda$) were scattered from the sample and collected on a two-dimensional detector (65 × 65 cm, 1 × 1 cm resolution). The available Q range extended from 0.0015 to 0.6 $Å^{-1}$.

The samples were measured at 25 °C in cylindrical quartz sample cells (NGS Precision) with a path length of 2 mm. The absolute scattering intensity, $I(Q)$, for each sample was obtained from the total detector counts corrected for background radiation, neutron transmission through the sample, scattering from the quartz cell, and detector sensitivity. The resulting scattering intensity versus scattering angle [$I(Q)$ versus Q] curves were fit to a polydisperse oblate cylinder form factor to determine the average aggregate size.[55]

Results and Discussion

Cumulative percentages of asphaltenes precipitated as a function of the overall solubility parameter in *n*-heptane/toluene mixtures are presented in Figure 2 for the various asphaltenes. Each data point in Figure 2 represents a different asphaltene fine fraction. The solubility parameter represented on the abscissa increases in proportion to the toluene volume fraction in the solvent blend for the fractionation. The ordinate represents the total amount of asphaltene material precipitated after the fractionation. The amount of a given asphaltene fine fraction may be determined from Figure 2 as the difference between the total amount of precipitated material from sequential

Table 3. Elemental Composition of *n*-Heptane-Soluble Asphaltene Fractions

parameter	B6	CS	HO
H/C	1.45	1.35	1.46
N/C	0.013	0.013	0.019
S/C	0.026	nd	nd
O/C	0.021	nd	nd
Na/C	2×10^{-5}	4×10^{-5}	2×10^{-5}
Ca/C	5×10^{-5}	3×10^{-5}	4×10^{-5}
K/C	1×10^{-5}	3×10^{-5}	1×10^{-5}
Mg/C	2×10^{-5}	2×10^{-5}	2×10^{-5}
V/C	6×10^{-4}	1×10^{-5}	2×10^{-4}
Al/C	3×10^{-5}	4×10^{-5}	3×10^{-5}
Fe/C	2×10^{-5}	2×10^{-5}	4×10^{-5}
Ni/C	4×10^{-5}	6×10^{-6}	6×10^{-5}

Table 4. Aggregate Sizes of *n*-Heptane-Soluble Fractions in Various Solvents

asphaltene	solvent	Rg (Å)
B6	toluene-*d*	19 ± 6
B6	90:10 methylnaphthalene-*d*/methanol-*d*	25 ± 6
HO	90:10 toluene-*d*/methanol-*d*	22 ± 8

fractionations. The final fractionation step in each of the experiments involved the precipitation from *n*-heptane. The *n*-heptane-soluble fractions for B6, CS, and HO asphaltenes consisted of 1.7, 3.9, and 3.0% of the whole asphaltenes, respectively. Because the individual fractions were characterized by the solubility parameter in which they precipitated, the chemical and colloidal properties of the *n*-heptane-soluble fractions were presented separately (Tables 3−4) from the remaining fractions (Figures 3−7).

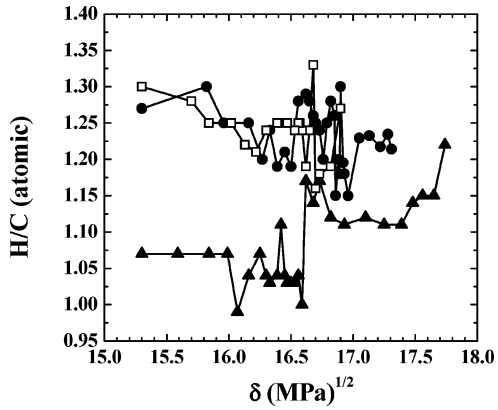

Figure 3. Variation in the atomic hydrogen/carbon ratio with total solubility parameters for (filled triangles) CS, (open squares) HO, and (filled circles) B6 asphaltene fractions.

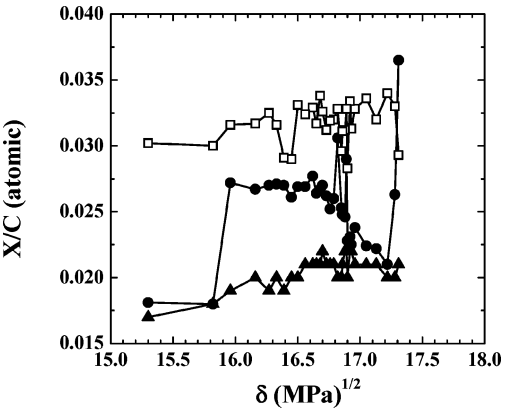

Figure 4. Variation in atomic (filled triangles) nitrogen/carbon, (filled circles) oxygen/carbon, and (open squares) sulfur/carbon ratios with total solubility parameters for B6 asphaltene fractions.

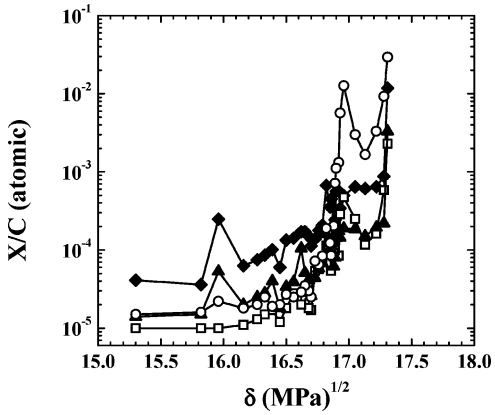

Figure 5. Variation in atomic (open circles) sodium/carbon, (filled diamonds) calcium/carbon, (open squares) potassium/carbon, and (filled triangles) magnesium/carbon ratios with total solubility parameters for B6 asphaltene fractions.

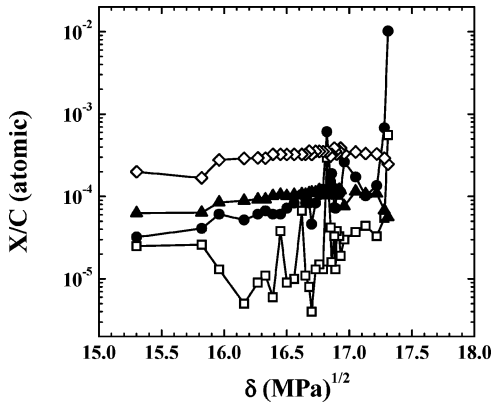

Figure 6. Variation in atomic (open diamonds) vanadium/carbon, (filled circles) aluminum/carbon, (open squares) iron/carbon, and (filled triangles) nickel/carbon ratios with total solubility parameters for B6 asphaltene fractions.

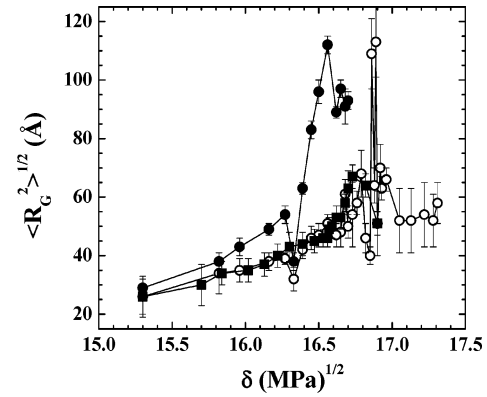

Figure 7. Variation in the aggregate size with the total solubility parameter for (open circles) B6 asphaltene fractions in 90:10 methylnaphthalene-*d*/methanol-*d*, (filled circles) B6 asphaltene fractions in toluene, and (filled squares) HO asphaltene fractions in 90:10 toluene-*d*/methanol-*d*.

The mass-weighted mean, standard deviation, and skewness of the elemental compositions were calculated assuming a Gaussian or "normal" distribution for the data sets, as shown in Table 5. For example, the weighted mean ($\bar{x}$) is given by[56]

$$\bar{x} = \frac{\sum_i w_i x_i}{\sum_i w_i} \tag{1}$$

where w_i and x_i are the mass fraction recovery of whole asphaltenes and the elemental composition of the fractions isolated at a given solubility parameter, i, respectively. Similarly, the weighted standard deviation (σ) and skewness (ζ) are given by

$$\sigma = \left[\frac{\sum_i w_i (x_i - \bar{x})^2}{\sum_i w_i}\right]^{1/2} \tag{2}$$

$$\zeta = \frac{\sum_i w_i (x_i - \bar{x})^3 / \sigma^3}{\sum_i w_i} \tag{3}$$

The calculations for the mass-weighted moments from eqs 1−3 excluded the elemental composition of the *n*-heptane-soluble fractions for the following reasons: (1) the elemental H/C and N/C ratios for these fractions varied by greater than 3σ from the mean values; (2) the individual fractions passed Chauvenet's criterion for rejecting the *n*-heptane-soluble samples from the data sets;[56] and (3) the solubility of these fractions in *n*-heptane suggests that they are not asphaltenes, by the definition used in this paper. The H/C and N/C ratios of the *n*-heptane-soluble fractions were chemically similar to resins obtained by saturates, aromatics, resins, and asphaltenes (SARA) fractionation of the crude oils (Table 2), suggesting that these fractions consisted of coprecipitated resins from the initial asphaltene precipitation.

Coefficients of linear correlation were calculated to determine if pairs of chemical and physical property data were linearly related, as shown in Tables 6−8. The correlation coefficient, r, between two sets of points, x and y, is defined by[56]

$$r = \frac{\sigma_{xy}}{\sigma_x \sigma_y} \tag{4}$$

where σ_{xy}, σ_x, and σ_y are the covariance and unweighted standard deviations in x and y, respectively. The covariance of N pairs of data points is given by

$$\sigma_{xy} = \frac{1}{N} \sum_i (x_i - x_{\text{mean}})(y_i - y_{\text{mean}}) \tag{5}$$

where x_{mean} and y_{mean} are calculated assuming equal weighting of the samples. Positive values of the correlation coefficient indicate that parameter y tends to increase as parameter x increases. Negative values indicate an inverse relationship. A stronger correlation of two data sets is indicated by larger values of $|r|$.

The variation in the atomic H/C ratios for the fine fractions as a function of the overall solubility parameter is shown in Figure 3. Values of the mean H/C ratio for the B6 and HO fractions (Table 5) agreed within 1σ of the H/C ratio for the whole asphaltenes (Table 2). This observation, coupled with a low skewness ($\zeta = 0.2$) of the data, suggests that the relative aromaticity of the fractions is "normally" distributed throughout the fractions. Aromaticity is likely not the driving force for precipitation of the HO and B6 fractions. A higher skewness ($\zeta = 1.2$) was observed in the H/C ratios for CS asphaltenes,

(56) Taylor, J. R. *An Introduction to Error Analysis: The Study of Uncertainties in Physical Measurements*; University Science Books: Sausalito, CA, 1982.

Table 5. Weighted Mean, Standard Deviation, and Skewness of Elemental Compositions (Excluding *n*-Heptane-Soluble Fractions)

	B6			CS			HO		
parameter	mean	standard deviation	skewness	mean	standard deviation	skewness	mean	standard deviation	skewness
H/C	1.21	0.04	0.2	1.04	0.04	1.2	1.24	0.04	0.2
N/C	0.021	0.001	−1.4	0.017	0.001	0.2	0.023	0.001	−0.8
S/C	0.032	0.001	−0.4	nd	nd	nd	nd	nd	nd
O/C	0.025	0.003	0.0	nd	nd	nd	nd	nd	nd
Na/C	1.0×10^{-3}	4.0×10^{-3}	5.1	6.0×10^{-5}	5.0×10^{-5}	4.4	2.0×10^{-4}	7.0×10^{-4}	6.6
Ca/C	4.0×10^{-4}	1.2×10^{-3}	9.2	4.0×10^{-5}	7.0×10^{-5}	10.5	9.0×10^{-5}	5.0×10^{-5}	5.4
K/C	1.0×10^{-4}	2.0×10^{-4}	7.3	4.0×10^{-5}	1.0×10^{-5}	0.4	1.0×10^{-5}	1.0×10^{-5}	5.6
Mg/C	1.0×10^{-4}	3.0×10^{-4}	9.1	2.0×10^{-5}	1.0×10^{-5}	4.7	2.0×10^{-5}	1.0×10^{-5}	5.6
V/C	1.1×10^{-3}	1.0×10^{-4}	−1.7	5.0×10^{-6}	5.0×10^{-6}	3.5	2.3×10^{-4}	4.0×10^{-5}	0.2
Al/C	2.0×10^{-4}	1.0×10^{-3}	9.5	5.0×10^{-5}	4.0×10^{-5}	3.1	6.0×10^{-5}	4.0×10^{-5}	5.7
Fe/C	3.0×10^{-5}	6.0×10^{-5}	7.3	2.0×10^{-5}	7.0×10^{-5}	13.5	2.0×10^{-5}	1.0×10^{-5}	1.0
Ni/C	1.1×10^{-4}	2.0×10^{-5}	−1.4	7.0×10^{-6}	1.2×10^{-5}	6.6	9.0×10^{-5}	1.0×10^{-5}	−0.1

Table 6. Correlation of Chemical Composition, Solubility, and Aggregate Size (in 90:10 Methylnaphthalene-*d*/Methanol-*d*) Parameters for B6 Asphaltenes

	δ	H/C	N/C	S/C	O/C	Na/C	Ca/C	K/C	Mg/C	V/C	Al/C	Fe/C	Ni/C	Rg
δ	1.000													
H/C	−0.332	1.000												
N/C	0.755	−0.381	1.000											
S/C	0.267	−0.157	0.381	1.000										
O/C	0.298	−0.082	0.282	0.010	1.000									
Na/C	0.451	−0.264	0.142	−0.128	0.424	1.000								
Ca/C	0.348	−0.094	0.049	−0.258	0.569	0.893	1.000							
K/C	0.439	−0.172	0.109	−0.202	0.514	0.971	0.966	1.000						
Mg/C	0.350	−0.106	0.059	−0.255	0.565	0.898	0.999	0.968	1.000					
V/C	0.501	−0.332	0.765	0.386	0.106	−0.334	−0.397	−0.360	−0.391	1.000				
Al/C	0.307	−0.078	0.026	−0.272	0.598	0.884	0.997	0.961	0.996	−0.414	1.000			
Fe/C	0.323	0.050	−0.002	−0.202	0.611	0.770	0.897	0.856	0.893	−0.320	0.902	1.000		
Ni/C	0.366	−0.231	0.651	0.283	−0.051	−0.525	−0.437	−0.486	−0.433	0.875	−0.460	−0.395	1.000	
Rg	0.530	−0.580	0.683	0.227	0.151	0.115	0.073	0.106	0.080	0.466	0.050	−0.005	0.475	1.000

Table 7. Correlation of Chemical Composition, Solubility, and Aggregate Size (in 90:10 Toluene-*d*/Methanol-*d*) Parameters for HO Asphaltenes

	δ	H/C	N/C	Na/C	Ca/C	K/C	Mg/C	V/C	Al/C	Fe/C	Ni/C	Rg
δ	1.000											
H/C	−0.404	1.000										
N/C	0.416	−0.312	1.000									
Na/C	0.374	−0.219	0.366	1.000								
Ca/C	0.500	−0.025	0.291	0.503	1.000							
K/C	0.362	−0.316	0.406	0.958	0.391	1.000						
Mg/C	0.441	0.014	0.276	0.480	0.995	0.369	1.000					
V/C	0.623	−0.210	0.237	0.536	0.495	0.521	0.443	1.000				
Al/C	0.401	0.056	0.225	0.419	0.981	0.295	0.980	0.430	1.000			
Fe/C	0.209	0.295	0.345	0.108	0.399	−0.016	0.393	0.319	0.395	1.000		
Ni/C	0.780	−0.370	0.279	0.412	0.420	0.423	0.357	0.942	0.342	0.285	1.000	
Rg	0.895	−0.515	0.249	0.410	0.311	0.403	0.242	0.645	0.186	0.167	0.810	1.000

Table 8. Correlation of Chemical Composition and Solubility Parameters for CS Asphaltenes

	δ	H/C	N/C	Na/C	Ca/C	K/C	Mg/C	V/C	Al/C	Fe/C	Ni/C
δ	1.000										
H/C	0.633	1.000									
N/C	0.520	0.317	1.000								
Na/C	0.489	0.712	0.059	1.000							
Ca/C	0.495	0.608	0.203	0.850	1.000						
K/C	0.001	0.137	−0.268	0.055	−0.186	1.000					
Mg/C	0.472	0.678	0.138	0.855	0.971	−0.098	1.000				
V/C	0.424	0.588	0.100	0.782	0.913	−0.056	0.929	1.000			
Al/C	0.451	0.566	0.352	0.564	0.704	−0.013	0.696	0.766	1.000		
Fe/C	0.408	0.518	0.197	0.774	0.977	−0.286	0.934	0.859	0.661	1.000	
Ni/C	0.275	0.360	0.320	0.330	0.511	−0.411	0.509	0.425	0.325	0.570	1.000

suggesting that the data do not necessarily obey a Gaussian distribution. The apparent step change in the average H/C ratio of CS asphaltenes near $\delta = 16.6$ $(\text{MPa})^{1/2}$ suggests that the earliest 10% of precipitated material is chemically different (i.e., less aromatic) than the remaining asphaltenes. To this extent, relative differences in aromaticity appear to drive the precipitation in CS asphaltenes. Upon precipitation of the initial 10% of CS asphaltenes, the remaining fractions did not vary significantly in the H/C ratio.

Relative trends in elemental composition of the B6 fractions were representative of trends in the HO and CS fractions, thus only B6 data was shown in Figures 4−6. Figure 4 shows the variation in atomic N/C, S/C, and O/C ratios for fractions of B6 asphaltenes. No measurements of elemental sulfur or oxygen were performed on the CS and HO fractions. As shown in Table 5, atomic S/C ratios of B6 asphaltenes appeared to obey a Gaussian distribution with slight negative skewness ($\varsigma = -0.4$). Sulfur content did not appear to be a driving force for asphaltene

precipitation. Atomic N/C ratios appeared to be "normally" distributed in the CS fractions, but higher negative skewness values were observed in the B6 and HO fractions. Figure 4 suggests that the earliest 90% (w/w) of B6 fractions to precipitate was normally distributed in nitrogen composition. The final 10% (w/w) of B6 asphaltenes that precipitated appeared to decrease in nitrogen composition with the decreasing solvent solubility parameter. This observation, coupled with considerably higher than average H/C ratios for the most soluble 10% (w/w) of B6 asphaltenes, suggests that these fractions are more chemically similar to the resin fraction than the bulk asphaltene fraction. In fact, the aggregation properties of the "resin"-like fractions as gauged by SANS are also distinctly different from those of the less soluble asphaltene fractions. Specifically, the degree of solvent entrainment of the resin-like fractions is very small or negligible, as compared to 30−50% for typical asphaltene fractions.[57] Additionally, the ratio of the average aggregate radius to the aggregate thickness (R_{avg}/L) of the polydisperse oblate cylinder fit to the resin-like fractions yields high values of 5−7 as compared to 1.5−4 for comparable asphaltene fractions.[57]

While the oxygen content of the B6 fractions (Table 5) appears to obey a Gaussian distribution, Figure 4 suggests that there is a systematic variation in the oxygen content of the fractions with a solubility parameter for the first ∼50% of asphaltenes to precipitate. The earliest precipitating fraction of B6 asphaltenes had a relatively high O/C ratio. The O/C ratios of the fractions precipitating between $\delta = 16.8$ and 17.2 $(MPa)^{1/2}$ generally increased with an increasing precipitated asphaltene yield. The most soluble 7% (w/w) of B6 asphaltenes had lower than average oxygen contents and were more "resin-like" in chemical composition.

Variations in atomic Na/C ratios of B6 asphaltene fractions are shown in Figure 5. The earliest fractions of B6 asphaltenes possessed relatively high concentrations of alkali and alkaline earth metals, particularly Na and Ca that accounted for 3.7 and 2.6% (w/w) of the fraction mass, respectively. The sums of the C, H, N, S, and O contents from the combustion of the first two B6 fine fractions were ∼71 and 82% (w/w), respectively. The incomplete combustion of the fractions, along with the enriched Na and Ca contents, suggests that a significant portion of the fractions contained coprecipitated metal oxides and inorganic salts. Atomic Na/C ratios of all asphaltene fractions appeared to decrease with decreasing δ, suggesting that most of the sodium-rich solids coprecipitated with the initial asphaltene fractions. A similar reduction in other alkali and alkaline earth metals contents (i.e., Ca/C, K/C, and Mg/C) was observed with a decreasing solubility parameter for the B6 fractions. As shown in Table 5, the distributions of alkali and alkaline earth metals contents in many instances had relatively large, positive values of the skewness parameter and values of the standard deviation that were larger than the calculated mean, suggesting that the data did not obey a Gaussian distribution.

Figure 6 and Table 5 indicate that the distribution of aluminum and iron contents in B6 asphaltenes is significantly skewed by the earliest precipitating fractions. Figure 4 indicates significantly higher oxygen contents in the earliest precipitating B6 fractions that coincided with higher than average aluminum and iron contents. Assuming that all of the Al and Fe species in the first B6 fine fraction were present as alumina and iron oxide (i.e., Al_2O_2 and Fe_2O_3), then oxygen in the form of metal oxides would account for approximately 0.96% (w/w) of the total chemical species. Normalized to the total carbon content in the first fraction, the atomic O/C ratio estimated for inorganic oxygen (∼0.013) was roughly the difference between the experimentally measured O/C ratio for the first fraction (∼0.037) and the mean O/C ratio for the B6 fractions (∼0.025). These results suggest the elevated oxygen content in the earliest B6 fine fractions was largely related to the presence of inorganic oxides that coprecipitated with the asphaltenes. Yang et al. observed a similar enrichment in the oxygen content of "fine solids" extracted from the earliest precipitating fraction of Athabasca asphaltenes in a 10:1 toluene/water mixture (v/v).[35]

Figure 6 also shows the general trends in vanadium and nickel contents of B6 asphaltenes during fractionation. As shown in Figure 6, V/C and Ni/C ratios appeared to vary randomly during the fractionation experiments. Neglecting the elemental compositions of the earliest precipitating fractions from the weighted moments analyses, the vanadium and nickel contents of the various fractions were more "normally" distributed than suggested in Table 5.

SANS measurements were performed on 1% (w/w) solutions of B6 fine fractions dispersed in mixtures of 90:10 methylnaphthalene-*d*/methanol-*d* (v/v) and in toluene-*d*. The HO fine fractions were dispersed in mixtures of 90:10 toluene-*d*/methanol-*d* (v/v). Aggregate average radii of gyration values, $\langle R_G^2 \rangle^{1/2}$, were obtained from nonlinear least-squares fits of the scattering intensity curves to a polydisperse oblate cylinder model.[55] Variation in the average aggregate size with the overall solvent solubility parameter is shown in Figure 7. Although the whole B6 asphaltenes were soluble in toluene at 1% (w/w), the earliest precipitated 65% of the whole asphaltenes did not redissolve in toluene at a similar concentration. B6 whole asphaltenes were previously observed to form aggregates of ∼50 Å in size in toluene-*d*.[10] As shown in Figure 7, the first toluene-soluble B6 fraction isolated at $\delta = 16.7$ $(MPa)^{1/2}$ formed aggregates of ∼93 Å in average size, suggesting that asphaltenes of the lower solubility parameter help solvate and reduce the aggregate size of asphaltenes with higher solubility parameters. This provides additional evidence of the synergistic interaction between "more soluble" and "less soluble" asphaltene fractions observed by Spiecker et al.[10] The average aggregate size in toluene-*d* generally decreased with a decreasing solubility parameter for the remaining B6 fractions. A small amount of methanol-*d* (i.e., 10%, v/v) was added to the solutions of B6 fine fractions in methylnaphthalene-*d* in an attempt to dissolve the less soluble fractions. The earliest precipitated B6 fraction and the two fractions that formed aggregates larger than 100 Å were not completely soluble in the 90:10 (v/v) mixture of deuterated methylnaphthalene/methanol. The aggregate sizes of the *n*-heptane-soluble fractions of B6 and HO in the selected solvents are shown in Table 4.

Table 6 shows the coefficients of linear correlation for various pairs of composition, solubility, and aggregate size parameters for B6 asphaltenes. Atomic N/C, H/C, and δ provided the highest correlations to the size of B6 aggregates in 90:10 methylnaphthalene-*d*/methanol-*d* mixtures with $r = 0.683$, −0.580, and 0.530, respectively. In comparison with the various parameters for elemental composition, the atomic H/C ratio correlated the most strongly with the nitrogen content. Table 6 also indicates a relatively high correlation of atomic N/C ratios with vanadium and nickel contents and suggests that a significant portion of the nitrogen functionality is bound in chelated porphyrin compounds. In fact, the maximum porphyrin nitrogen fraction can be estimated from the vanadium and nickel

(57) (a) Gawrys, K. L.; Kilpatrick, P. K. *Langmuir*, manuscript submitted for publication. (b) Gawrys, K. L. Ph.D. Thesis, North Carolina State University, Raleigh, NC, 2005.

concentrations in the asphaltenes by assuming that all of the vanadium and nickel are distributed in porphyrin structures.[58] Previous UV−vis spectroscopic analyses of whole crude oil and bitumen samples in the Soret region (~410 nm) suggest that only 40−60% of vanadium species are generally present in porphyrin complexes;[59−60] therefore, only the maximum value is calculated. The maximum fraction of nitrogen associated with porphyrin groups for B6, HO, and CS asphaltene fractions ranged from 5 to 10%, 4 to 8%, and less than 0.7%, respectively. Thus, potentially high correlations of N, V, and Ni contents are expected for B6 and HO asphaltenes but not CS asphaltenes. The correlation coefficients in Table 6 were consistent with previous studies that indicated that the size of aggregates in solution generally increased with increasing aromaticity and N/C content of the asphaltene fractions[13,49] and suggest the importance of metalloporphyrins in the asphaltene aggregation mechanism. Similarly, Table 7 indicates that the size of HO aggregates in 90:10 toluene-*d*/methanol-*d* was highly correlated to nickel and vanadium contents but not atomic nitrogen. Relative to B6 asphaltenes, the weaker correlation of atomic N/C with nickel and vanadium in HO asphaltenes suggests that a smaller fraction of the atomic nitrogen is bound to metalloporphyrin functional groups.

Aggregate sizes were not determined for CS asphaltenes in similar solvents; however, it was observed that CS asphaltenes were not generally soluble in 90:10 methylnaphthalene-*d*/methanol-*d*. Table 8 indicates that atomic H/C and N/C ratios were not highly correlated ($r = 0.317$). The relatively low concentrations of vanadium and nickel in the CS asphaltene fractions (Table 5) coupled with the relatively poor correlation of these parameters suggest that metalloporphyrin content is not the driving force for aggregation in CS asphaltenes. Furthermore, the addition of methanol-*d* to solutions of CS asphaltenes in methylnaphthalene-*d* likely induced asphaltene precipitation, because these fractions had a lower concentration of polar nitrogen than B6 and HO asphaltenes. These results are consistent with previous fractionation studies that concluded that aggregation in CS asphaltenes was dominated by π-bonding interactions, while polar interactions drove aggregation in B6 and HO asphaltenes.[13]

The oxygen content in B6 asphaltenes was more highly correlated to various metals contents (e.g., Fe and Al) than hydrogen, nitrogen, or sulfur (Table 6). Tables 6−8 also indicate relatively high correlations between alkali and alkaline earth metals, iron, and aluminum contents. These observations further support the claim that inorganic oxides and other "fine" solids likely coprecipitated with the asphaltenes during fractionation. On the basis of the correlation of solubility parameters with chemical composition, the major driving force for precipitation of B6 asphaltenes appears to be the nitrogen content with secondary importance to the vanadium content (Table 6). Vanadium and nickel showed the highest correlation to the solubility parameter of HO asphaltenes (Table 7). These results suggest that polar and hydrogen-bonding interactions are more important than dispersion interactions for the precipitation of HO and B6 asphaltenes from mixtures of *n*-heptane and toluene. On the other hand, the H/C ratio appears to correlate more strongly to the solubility parameter than other elemental contents for CS asphaltenes (Table 8), suggesting a greater importance of dispersion interactions in this crude oil.

(58) Mitra-Kirtley, S.; Mullins, O. C.; van Elp, J.; George, S. J.; Chen, J.; Cramer, S. P. *J. Am. Chem. Soc.* **1993**, *115*, 252.

(59) Reynolds, J. G. In *Asphaltenes and Asphalts, 2*; Yen, T. F., Chilingarian, G. V., Eds.; Elsevier: New York, 2000; p 42.

(60) Strong, S.; Filby, R. H. In *Metal Complexes in Fossil Fuels*; Filby, R. H., Branthaver, J. F., Eds.; ACS Symposium Series Number 344, American Chemical Society: Washington, DC, 1987; p 168.

Conclusions

Asphaltenes from three different crude sources were fractionated into 20−30 discrete fractions by sequential precipitation in mixtures of *n*-heptane and toluene. Sufficient asphaltene material was isolated during each fractionation to perform subsequent chemical analyses and SANS studies on the fractions. An *n*-heptane-soluble fraction, similar in chemical composition and aggregation behavior to petroleum resins, was generated during the final fractionation step. ICP metals analyses suggested that the fractions contained significant amounts of inorganic fine solids (e.g., metal oxides and salts) that coprecipitated with the asphaltene species. Most of the inorganic solids appeared to precipitate with the earliest fractions, with the small concentration of material remaining precipitating randomly during the later fractionations. The "early" precipitation of many of the inorganic solids tended to skew the distribution of many of the metals to values higher than the mean of a "normal" distribution. In fact, weighted statistical analyses suggested that most of the metals contents of the fractions did not obey a Gaussian distribution. Atomic H/C and N/C ratios in the earliest precipitated ~90% of B6 and HO asphaltenes appeared to obey a Gaussian distribution, with mean values approximating the average values for the whole asphaltenes. The sulfur content also appeared to be normally distributed in B6 asphaltenes. CS asphaltenes showed an apparent bimodal distribution of atomic H/C ratios because the initial 10% of precipitated material was generally less aromatic than the remaining asphaltenes.

SANS experiments in mixtures of toluene-*d* (or methylnaphthalene-*d*) and methanol-*d* suggested that aggregate size generally decreased with a decreasing solubility parameter. Deuterated methanol was used as a cosolvent in these experiments to assist the dissolution of the earliest precipitating fractions; however, the solvent behaved as a flocculant for the CS asphaltene fractions.

Coefficients of linear correlation for the chemical composition, solubility, and aggregate size parameters provided a statistical means of determining the properties of the asphaltene fractions that promoted aggregation and precipitation. The observation that aggregation in B6 asphaltenes was most highly correlated to atomic N/C and H/C ratios was consistent with previous scattering experiments. The nitrogen content also provided the highest correlation to the solubility parameter in B6 asphaltenes. The relatively high correlation of the N/C ratio with vanadium and nickel contents in B6 asphaltenes suggests that interactions of chelated porphyrin compounds are important in the asphaltene aggregation mechanism. In fact, vanadium and nickel contents provided the highest correlation to the aggregate size and solubility parameter in HO asphaltenes.

On the basis of these results, polar and hydrogen-bonding interactions appear to be more important than dispersion interactions in the precipitation of B6 and HO asphaltenes from mixtures of *n*-heptane and toluene. In particular, interactions of metalloporphyrins appear to play a key role in the asphaltene aggregation mechanism. On the other hand, low concentrations of nitrogen, vanadium, and nickel were observed in the CS asphaltene fractions relative to the B6 and HO fractions. The atomic H/C ratio provided the highest correlation to the solubility parameter for CS asphaltenes. The role of dispersion interactions was likely more important than polar and hydrogen-bonding interactions in determining the solubility of CS asphaltenes.

Acknowledgment. This research is supported by the Petroleum Environmental Research Forum, ExxonMobil, Shell, Equilon, ChevronTexaco, Nalco Energy Services Division, Champion Technologies, National Science Foundation Grant (CTS981727), and the NSF Graduate Research Fellowship Program. We acknowledge Darlene Mahlow at the University of Alberta for performing combustion elemental analyses on the asphaltene and resin samples. Additional combustion elemental analyses and ICP metals analyses were performed by Rebecca L. Ramsey at Nalco Energy Services in Sugar Land, TX. This work benefited from the use of facilities in the Intense Pulsed Neutron Source and the Chemistry Division, which is funded by the U.S. Department of Energy, Office of Basic Energy Sciences, under contract W-31-109-ENG-38 to the University of Chicago. We particularly thank Pappannan Thiyagarajan and Denis Wozniak of the Intense Pulsed Neutron Source Division at Argonne National Laboratory for their assistance with the SAND instrument. We also acknowledge the support of the National Institute of Standards and Technology, U.S. Department of Commerce, in providing the neutron research facilities used in this work and Min Lin for his assistance on the NG1 and NG3 beamlines. We also thank Matthew B. Smith, M. Lupe Marques, and Vincent Verruto for helping with the sample preparation and SANS data collection.

EF0502002